Hippocampus / Volume 29, Issue 11

RESEARCH ARTICLE | Full Access

TRPC channels are not required for graded persistent activity in entorhinal cortex neurons

Alexei V. Egorov, Dagmar Schumacher, Rebekka Medert, Lutz Birnbaumer, Marc Freichel, Andreas Draguhn

First published: 19 April 2019
https://doi-org.ezproxy.nihlibrary.nih.gov/10.1002/hipo.23094

Marc Freichel and Andreas Draguhn shared senior authorship.

Funding information: Deutsche Forschungsgemeinschaft, Grant/Award Numbers: FOR 2289, P02 , SFB 1118, B02, SFB 1134, A01, SFB/Transregio 152, P07, P21; NIH Intramural Research Program, Grant/Award Number: Z01-ES-101684

Abstract

Adaptive behavior requires the transient storage of information beyond the physical presence of external stimuli. This short-lasting form of memory involves sustained ("persistent") neuronal firing which may be generated by cell-autonomous biophysical properties of neurons or/and neural circuit dynamics. A number of studies from brain slices reports intrinsically generated persistent firing in cortical excitatory neurons following suprathreshold depolarization by intracellular current injection. In layer V (LV) neurons of the medial entorhinal cortex (mEC) persistent firing depends on the activation of cholinergic muscarinic receptors and is mediated by a calcium-activated nonselective cation current (I_{CAN}). The molecular identity of this conductance remains, however, unknown. Recently, it has been suggested that the underlying ion channels belong to the canonical transient receptor potential (TRPC) channel family and include heterotetramers of TRPC1/5, TRPC1/4, and/or TRPC1/4/5 channels. While this suggestion was based on pharmacological experiments and on effects of TRP-interacting peptides, an unambiguous proof based on TRPC channel-depleted animals is pending. Here, we used two different lines of TRPC channel knockout mice, either lacking TRPC1-, TRPC4-, and TRPC5-containing channels or lacking all seven members of the TRPC family. We report unchanged persistent activity in

mEC LV neurons in these animals, ruling out that muscarinic-dependent persistent activity depends on TRPC channels.

1 INTRODUCTION

Working memory represents the ability of neuronal networks to maintain information for short periods of time after disappearance of the triggering stimulus. This transient storage may involve sustained ("persistent") neuronal firing during the delay period, as suggested by different studies in nonhuman primates (Funahashi, Bruce, & Goldman-Rakic, 1989; Miller, Erickson, & Desimone, 1996; Romo, Brody, Hernández, & Lemus, 1999), humans (Kamiński et al., 2017), and rodents (Harvey, Coen, & Tank, 2012; MacDonald, Lepage, Eden, & Eichenbaum, 2011; Pastalkova, Itskov, Amarasingham, & Buzsaki, 2008). Memory-associated persistent firing has been observed in multiple brain areas, including cortical networks, for example, prefrontal, parietal, inferior temporal, auditory, somatosensory, and entorhinal cortex (EC) (Zylberberg & Strowbridge, 2017). Persistent activity may be caused by cell-autonomous (intrinsic) biophysical properties, neural circuit dynamics (i.e., synaptic reverberation in recurrent circuits) or a combination of both (Major & Tank, 2004; Zylberberg & Strowbridge, 2017). A number of studies from brain slices reports that suprathreshold depolarization by intracellular current injection can initiate firing that outlasts the stimulus even during pharmacological blockade of synaptic transmission. Such intrinsically generated persistent firing has been observed in excitatory neurons of prefrontal cortex (Lei et al., 2014), perirhinal cortex (Navaroli, Zhao, Boguszewski, & Brown, 2012), EC (Egorov, Hamam, Fransén, Hasselmo, & Alonso, 2002; Tahvildari, Fransén, Alonso, & Hasselmo, 2007), amygdala (Egorov, Unsicker, & von Bohlen und Halbach, 2006), postsubiculum (Yoshida & Hasselmo, 2009), and hippocampus (Jochems & Yoshida, 2013; Knauer, Jochems, Valero-Aracama, & Yoshida, 2013; Larimer & Strowbridge, 2010). Persistent activity in the medial entorhinal cortex (mEC) is mediated by a calcium-activated nonselective cation current (I_{CAN}) (Egorov, Hamam, et al., 2002; Fransén, Tahvildari, Egorov, Hasselmo, & Alonso, 2006; Tahvildari, Alonso, & Bourque, 2008). It has been suggested that the channels underlying I_{CAN} in mEC layer V (LV) neurons belongs to the transient receptor potential (TRP) channel family (Al-Yahya, Hamel, Kennedy, Alonso, & Egorov, 2003), specifically to the canonical TRP channel subfamily (TRPC) (Reboreda, Jiménez-Díaz, & Navarro-López, 2011; Zhang, Reboreda, Alonso, Barker, & Séguéla, 2011). Indeed, the seven members of TRPC subfamily (TRPC1–TRPC7) form nonselective cation channels that are activated in response to stimulation of phospholipase C-coupled receptors (Montell, Birnbaumer, & Flockerzi, 2002; Wu, Sweet, & Clapham, 2010). These properties are apparently in line with the observed muscarinic receptor-dependent persistent activity in EC LV neurons (Egorov, Hamam, et al., 2002), which has been suggested to be mediated heterotetramers consisting of either TRPC1 and TRPC5, TRPC1 and TRPC4 and/or TRPC1 with TRPC4 and TRPC5 channels (Zhang et al., 2011). Recently, we analyzed the assembly of TRPC1, TRPC4, and TRPC5 in the central nervous system by means

of quantitative high-resolution mass spectrometry (Bröker-Lai et al., 2017). Indeed, affinity purifications of TRPC isoforms from mouse hippocampal membranes antibodies demonstrated robust coassembly of TRPC1, TRPC4, and TRPC5, while no other TRP channels were detected. Thus, TRPC1/4/5 channels form heteromers from three (TRPC1–TRPC4–TRPC5) or two subunits (TRPC1–TRPC4, TRPC1–TRPC5, TRPC4–TRPC5) (Bröker-Lai et al., 2017). Despite such insights about the molecular composition of TRPC subunits, the functional contribution of TRPC channels to intrinsic neuronal properties is less clear. Based on pharmacological experiments using flufenamic acid (100 μM), 2-APB (100 μM), or SKF-96365 (50 μM) and on effects of TRPC4/TRPC5-interacting peptides TRPC channels have been proposed to mediate sustained neuronal firing (Zhang et al., 2011). However, an unambiguous proof based on TRPC channel-depleted animals is pending.

Here, we used two different lines of TRPC channel knockout (KO) mice, either lacking TRPC1-, TRPC4-, and TRPC5-containing channels (Bröker-Lai et al., 2017) or lacking all seven members of the TRPC family (Birnbaumer, 2015). We report unchanged persistent activity in mEC LV neurons in these animals, ruling out that muscarinic-dependent persistent activity depends on TRPC channels.

2 MATERIALS AND METHODS

2.1 Animals

Experiments were performed using male TRPC1/4/5-triple-KO and TRPC1/2/3/4/5/6/7-hepta-KO mice. All experimental procedures were approved and performed in accordance with the ethic regulations and the animal welfare committee of Heidelberg University and with the approval of the state government of Baden-Wüurttemberg. Housing was provided in Makrolon II cages with a maximum of three animals in a temperature-controlled holding room (23 ± 1°C) on a 12/12-hr light/dark cycle. Animals had ad libitum access to food and water.

A triple-KO mouse line Trpc1/4/5−/− lacking TRPC1, TRPC4, and TRPC5 was generated by intercrossing mice of the three mouse lines Trpc1−/− (Dietrich et al., 2007), Trpc4−/− (Freichel et al., 2001), and Trpc5−/− (Xue et al., 2011). Each had been backcrossed to the C57Bl6/N strain (Charles River) for at least seven generations before they were used to generate the Trpc1/4/5−/− line. For all details see (Bröker-Lai et al., 2017).

The hepta-KO mouse line Trpc1/2/3/4/5/6/7−/− lacking all seven TRPC subtypes (TRPC1, TRPC2, TRPC3, TRPC4, TRPC5, TRPC6, TRPC7) was generated by intercrossing mice of the following mouse lines: Trpc1−/− (Dietrich et al., 2007), Trpc2−/− (Stowers, Holy, Meister, Dulac, & Koentges, 2002), TRPC3−/− (Hartmann et al., 2008), Trpc4−/− (Freichel et al., 2001), Trpc5−/− (Phelan et al., 2013), Trpc6−/− (Dietrich et al., 2005), and Trpc7−/− (Perez-Leighton, Schmidt, Abramowitz, Birnbaumer, & Kofuji, 2011). Trpc1/2/3/4/5/6/7−/− (hepta-TRPC KO) mice are

viable and fertile (Birnbaumer, 2015). First generation (F1) offspring of C57Bl6/N and 129SvJ intercrosses were used as wild type (WT) controls for Trpc1/2/3/4/5/6/7−/− mice that were also on mixed genetic background derived from C57 and 129 strains. All mice used in experiments were genotyped for deficiency in Trpc alleles (for details see Figure S1 and Table S1).

2.2 Preparation of mouse brain slices

Horizontal brain slices (450 μm thick) containing the hippocampus and EC were obtained from 3 to 4 month old mice using standard techniques (Roth, Beyer, Both, Draguhn, & Egorov, 2016). To minimize animal suffering, we decapitated mice under deep CO_2-induced anesthesia and used up to six slices per animal for experiments. After decapitation, brains were rapidly removed and placed in cold (1–4°C) oxygenated artificial cerebrospinal fluid (ACSF) containing (in mM): 124 NaCl, 3 KCl, 1.8 $MgSO_4$, 1.6 $CaCl_2$, 10 glucose, 1.25 NaH_2PO_4, 26 $NaHCO_3$, saturated with carbogen (95% O_2/5% CO_2, pH 7.4 at 34°C). Brain slices were cut using a vibratome slicer (Leica VT1200S, Nussloch, Germany), then transferred into a Haas-type interface chamber (Haas, Schaerer, & Vosmansky, 1979), superfused with ACSF at a rate of 1.5–2 mL/min, and maintained at 34 ± 1°C. Prior to electrophysiological recordings, slices were allowed to recover for at least 2 hr.

2.3 Recording procedures

Intracellular recordings were obtained using sharp microelectrodes pulled on a Flaming/Brown puller P-1000 (Sutter Instruments, Novato, CA) from 1.5 mm borosilicate glass capillaries (Science Products, Hofheim, Germany, Cat. No. GB150F-10). Electrodes were filled with 2 M K-acetate containing 1% biocytin (Sigma-Aldrich, Taukirchen, Germany, Cat. No. B4261) (tip resistance of 70–110 MΩ). We used biocytin staining to confirm cell location after the experiment. Potentials were amplified using an Axoclamp-2 amplifier (Axon Instruments, Burlingame, CA), filtered at 3 kHz and digitized at 20 kHz with an ADC (model MICRO 1401 mkII, CED, Cambridge, UK). Signals were stored on a computer and visualized using Spike2 software (CED, Cambridge, UK). Intracellular potentials were recorded in bridge mode and the bridge balance was monitored throughout the experiment. Durations of positive and negative current injections (range 0.1–0.8 nA) were controlled using a Master-8 VP stimulator (AMPI, Jerusalem, Israel). Membrane potential was manually adjusted by intracellular injection of DC current through the recording electrode and held near firing threshold (approximately −60 mV) for suprathreshold conditions. The mEC was identified with a dissecting microscope by transillumination. EC LV excitatory neurons were identified electrophysiologically on the basis of their firing characteristics as previously described (Egorov, Heinemann, & Müller, 2002; Hamam, Kennedy, Alonso, & Amaral, 2000).

2.4 Chemicals

Carbachol (CCh, 10–20 μM, Cat. No. C4382) and atropine (10 μM, Cat. No. A0257, both from Sigma-Aldrich, Taufkirchen, Germany) were bath-applied by continuous perfusion. As the muscarinic-induced phenomena did not desensitize, the neurons were directly impaled in the presence of CCh. All recordings were performed during blockade of ionotropic glutamate- and GABA-mediated neurotransmission with a drug mixture consisting of a cocktail of DL-2-amino-5-phosphonovaleric acid (APV, 30 μM, Tocris Bristol, UK, Cat. No. 0105), 6-cyano-7-nitroquinoxaline-2,3-dione (CNQX, 10 μM, Tocris Bristol, UK, Cat. No. 1045), and picrotoxin (100 μM, Sigma-Aldrich, Taufkirchen, Germany, Cat. No. P1675). Picrotoxin was applied from stock solution made in DMSO. The final concentration of DMSO in ACSF was ≤0.1%.

2.5 Data analysis

Electrophysiological data were analyzed using Spike 2 laboratory software. Spectral (Fourier) analysis and peristimulus histograms were made using Spike 2. Averaged data are given as mean ± *SD* or as median and the first and third quartiles (P_{25} and P_{75}). Calculation of the statistical significance was performed using unpaired, two-tailed Student's *t* test for normally distributed data or Mann–Whitney *U* test for non-normally distributed data. Statistical analysis was performed using GraphPad (InStat, San Diego, CA) software. Regression analysis was performed using simple linear regression in GraphPad (InStat, San Diego, CA), quantified by correlation coefficient r^2.

Intrinsic properties of neurons are summarized in Table S2. All values were obtained in the presence of CCh and during blockade of AMPA-, NMDA-, and GABA(A)-mediated neurotransmission. Resting membrane potential (RMP) was estimated by subtraction of the tip potential following withdrawal of the pipette from the cell. Input resistance was determined at RMP by passing current pulses (−0.2 nA, 200 ms) through the recording electrode and measuring the resulting voltage deflections (at late steady-state level). For the analysis of action potential (AP) properties, we injected DC current with slowly rising amplitude until the cell started firing at low frequency. AP threshold was calculated as the first peak of the second derivative. AP amplitude was calculated as difference between the membrane voltage at AP threshold and AP peak. AP half-width was measured at the membrane voltage halfway between AP threshold and AP peak. AP maximum rise slope was calculated as maximum of the first derivative of membrane voltage between AP threshold and AP peak. AP maximum repolarization slope was calculated as maximal negative amplitude of the first derivative of membrane voltage following AP peak. Fast afterhyperpolarization (fAHP) following single AP was determinated from the notch at the end of the fast repolarization phase within 5 ms after AP peak. fAHP amplitude was calculated as difference between AP threshold and the notch potential. Amplitude of medium afterhyperpolarization (mAHP) was calculated similarly from the time interval of 5–50 ms after AP peak. Trains of APs were induced by positive current injection of 1 s duration starting from ~12 mV negative to spike threshold. In this case,

amplitude of the resulting mAHP was calculated as difference between minimum membrane voltage within 200 ms after current-step offset and AP threshold or recording membrane potential, as indicated. The frequency of persistent firing was calculated as average value from at least 20 s of recording. During persistent spiking, membrane potential oscillates between afterhyperpolarizations and spikes. We typically observed a short inflection (or plateau) immediately prior to the AP. These potentials were taken as estimated membrane potential during persistent firing and were compared to baseline potential to calculate the depolarization during persistent firing.

2.6 Expression analysis by quantitative PCR

For quantitative PCR (qPCR) analysis of the expression of Trpc1–Trpc7 transcripts in the EC (Figure 2a) horizontal brain slices (1,800 µm thick) were obtained from 3 to 4 month old mice (F1, see section animals) using standard procedures as described above. Area of interest (the EC together with the perirhinal and postrhinal cortices; see Figure 2a right) was dissected from individual slices under visual control (two slices pro animal; i.e., one slice from each brain hemisphere). Tissue was placed into greiner bio-one tubes, cooled with liquid nitrogen and then stored at −80°C. For RNA isolation tissue was homogenized in Qiagen's RLT buffer first by using a Polytron (Kinematica PT 1200 E), followed by a glass homogenizer (Kimble Kontes Tenbroeck 2 mL) and centrifugation in the QIAshredder column according to manufacturer's recommendations. RNA isolation was performed using the RNeasy Mini kit (Qiagen) according to manufacturer's recommendations for tissue, including on-column DNase digest. cDNA synthesis was carried out using the SensiFAST cDNA synthesis kit (Bioline) according to manufacturer's recommendations. Primers were designed with the online tool provided by Roche (https://lifescience.roche.com/en_de/brands/universal-probe-library.html) and the best primer pair for each target out of 2–3 was chosen from an initial qPCR screen. Quantitative expression analysis was performed using the Universal Probe system (Roche) with the corresponding FastStart Essential DNA Probes Master (Roche) on a LightCycler 96 Instrument (Roche, Mannheim, Germany). Relative expression levels were obtained by normalizing to H3 histone family member 3A (H3F3A), aryl-hydrocarbon receptor-interacting protein (AIP), and CXXC finger protein 1 (CXXC1) expression levels. Primer sequences are listed in Table 1.

Table 1. Primer sequences used for qPCR analysis with FastStart essential DNA probes

		Primer sequence	Probe
TRPC1	Fw	agggtacacttccaaagagcag	105
	Rev	ccaatgaacgagtggaaggt	
TRPC2	Fw	tccttgtcttcctcggagtc	52

		Primer sequence	Probe
	Rev	ttcacagatagggcactggac	
TRPC3	Fw	aagttcatggttctcttcattatgg	72
	Rev	gaataaagtatgaacatgccaatca	
TRPC4	Fw	ggaatcatgggacatgtgg	53
	Rev	cggagggaactgaagatgttt	
TRPC5	Fw	gtggattcacggaatacatcc	31
	Rev	ttgccaggtagagggagttc	
TRPC6	Fw	cggggagagactgtcgttag	78
	Rev	gaggggctctgctctatctg	
TRPC7	Fw	gctcatcatgaagtgggtctta	93
	Rev	tcctcccagatctccttgc	

Reference genes

		Primer sequence	Probe
H3F3A	Fw	gccatctttcaattgtgttcg	19
	Rev	agccatggtaaggacacctc	
AIP	Fw	cgcctgtggtaagcagaga	29
	Rev	aagcgagctttgtcctcct	
CXXC1	Fw	tagtgccgaccgctgact	26
	Rev	ggcctctcccctaactgaat	

Abbreviation: qPCR, quantitative PCR.

For analysis of the expression of Trpc1–Trpc7 transcripts in hepta-TRPC KO tissue as compared to control mice (Figure 2b), we designed the primer pairs listed in Table 2. For each intron spanning assay one primer was located in the exon that was deleted in the corresponding Trpc

genes, and the second primer was placed in the adjacent exon upstream or downstream of the deleted exon. Quantitative expression analysis was performed using RNA obtained from frontal lobes of the brain of four independent hepta-TRPC KO mice and WT controls, respectively. The amplification reaction was performed using the iTaq Universal SYBR® Green Supermix (Bio Rad) on a LightCycler 96 Instrument (Roche, Mannheim, Germany). Expression levels are displayed as Cq values (limited to 35 cycles) for each of the seven Trpc genes in comparison to the H3F3A, AIP, and CXXC1 housekeeping genes.

Table 2. Primer sequences used for qPCR analysis with iTaq universal SYBR® green

		Primer sequence
TRPC1	Fw	acctttgccctcaaagtggt
	Rev	gcccaaaatagagctggttg
TRPC2	Fw	cgctccaagctctacctgtc
	Rev	ggatggcaggatgttaaagg
TRPC3	Fw	cctgcttttaccacggttga
	Rev	ctgtcatcctcgatctcttgg
TRPC4	Fw	ggaatcatgggacatgtgg
	Rev	cggagggaactgaagatgttt
TRPC5	Fw	gtggattcacggaatacatcc
	Rev	ttgccaggtagagggagttc
TRPC6	Fw	tgacaaaagtcacactgggg
	Rev	ggatcagtagggtcccactt
TRPC7	Fw	gctcatcatgaagtgggtctta
	Rev	tcctcccagatctccttgc

Reference genes		Primer sequence
H3F3A	Fw	gccatctttcaattgtgttcg

Reference genes		
		Primer sequence
	Rev	accagtcatccaccaagagg
AIP	Fw	aggcgatggcgtcatagta
	Rev	aagcgagctttgtcctcct
CXXC1	Fw	tagtgccgaccgctgact
	Rev	ggcctctcccctaactgaat

Abbreviation: qPCR, quantitative PCR.

3 RESULTS

3.1 Persistent activity in TRPC1/4/5-triple-KO mice

Muscarinic-dependent plateau potential and persistent activity in EC LV neurons are mediated by a calcium-activated nonselective cation current (I_{CAN}) (Egorov, Hamam, et al., 2002; Fransén et al., 2006). TRP channels are permeable to both monovalent and divalent cations and are promising candidates underlying I_{CAN} (Ramsey, Delling, & Clapham, 2006). Indeed, there is pharmacological evidence that I_{CAN} is mediated by TRP channels in the mEC (Al-Yahya et al., 2003; Reboreda et al., 2011). These channels are likely composed of the canonical channel subunits TRPC1, TRPC4, and TRPC5 (Zhang et al., 2011). However, a more direct proof using genetic interventions is missing. We therefore recorded intracellular potentials from individual mEC LV neurons of mice lacking the implicated channel subunits (Trpc1/Trpc4/Trpc5-triple-KO; TRPC1/4/5 KO; Bröker-Lai et al., 2017). Sharp microelectrode recordings were performed from EC slices of TRPC1/4/5 KO mice in the presence of the cholinergic receptors agonist CCh (10–20 μM) and during blockade of AMPA-, NMDA-, and GABA(A)-mediated neurotransmission. Under these conditions the RMP was −65.3 ± 1.2 mV (n = 8) and average input resistance was 66 ± 27 MΩ (n = 8). Intrinsic properties of neurons are summarized in Table S2. To our surprise, we found that all tested mEC LV neurons from TRPC1/4/5 KO mice (eight neurons from four mice) were able to generate persistent firing: neurons responded to a suprathreshold current-step stimulus with delayed firing at a constant frequency (4.5–14 Hz) for an apparently indefinite period of time (tested up to 5 min) (Figure 1). Stimulation parameters required to elicit persistent activity varied from cell to cell. In general, positive current injections of 1–4 s duration starting from ~12 mV or less negative to spike threshold and eliciting spike trains of 20

–51 Hz were sufficient. Similar to our previous observations in rats (Egorov, Hamam, et al., 2002; Egorov et al., 2006), persistent firing displayed pronounced activity- and voltage-dependence (i.e., the probability to induce sustained firing activity increased with rising duration/intensity of stimulation and with membrane depolarization, and vice versa). Figure 1 illustrates an example recording where current pulses of different duration were applied at a given voltage level. At this voltage level stimulation for 1 or 2 s triggered only after-depolarizations or prolonged plateau potentials. Increasing stimulus duration, however, led to a stable state of sustained spiking (Figure 1, left). After membrane hyperpolarization, trigger pulses of equivalent strength were not able to induce persistent firing (Figure 1, right). In the same neurons persistent firing could be elicited by a short stimulation from more depolarized voltage levels at about 10 mV or less negative to spike threshold. Thus, a stimulation with 1 s long suprathreshold current-step (spike train at 44.5 ± 5 Hz) caused sustained firing at a frequency of 9.0 ± 3.6 Hz in all tested cells (n = 8/8). The sustained firing was accompanied by a poststimulus persistent depolarization of 4.1 ± 1.3 mV (n = 8) measured as the difference between the estimated membrane potential during persistent firing and the baseline potential before its induction (see Section 2.5). The quantitative parameters of persistent activity are summarized in Table 3. In two out of four neurons persistent firing could be induced with strong current steps of 0.2 s duration (spike train frequency during stimulation was 70–85 Hz). Together, this data shows the ability of EC LV neurons to generate persistent activity in the absence of TRPC1-, TRPC4-, and TRPC5-containing channels.

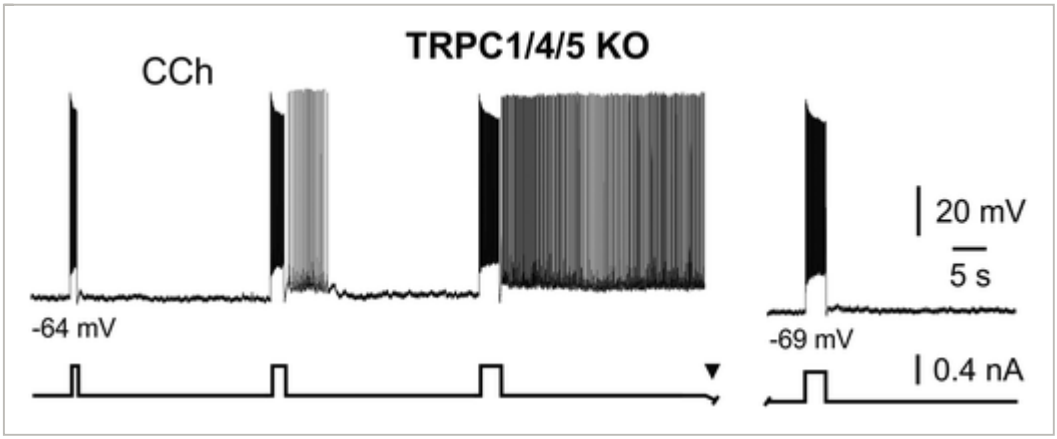

Figure 1

Open in figure viewer | PowerPoint

CCh-induced persistent firing in TRPC1/4/5-triple-knockout mice. Responses of mEC LV neuron to depolarizing current steps of different duration (left). Current pulse of equivalent strength was not able to elicit persistent firing after slight membrane hyperpolarization (right). Recording was obtained during blockade of neurotransmission with CNQX (10 μM), APV (30 μM), and picrotoxin (100 μM). APV, DL-2-amino-5-phosphonovaleric acid; CCh, carbachol; CNQX, 6-cyano-7-

nitroquinoxaline-2,3-dione; LV, layer V; mEC, medial entorhinal cortex; TRPC, transient receptor potential canonical

Table 3. The quantitative parameters of persistent activity in mEC LV neurons of TRPC1/4/5 knockout mice, and hepta-TRPC knockout versus WT control mice

mEC LV	**TRPC1/4/5 KO**		**Hepta-TRPC KO**		**Versus**		**WT control**	
		n		***n***	***p***	***Test***		***n***
1 s current step								
Persistent firing (neurons)	8 out of 8		8 out of 11				6 out of 6	
Initiation firing (Hz)	44.5 ± 5.0	8	32.9 ± 5.8	8	0.113	*t* test	37.4 ± 3.3	6
Persistent firing (Hz)	9.0 ± 3.6	8	6.7 ± 3.7	8	0.253	*t* test	8.7 ± 2.3	6
Post. stim. depolarization (mV)	4.1 ± 1.3	8	4.4 ± 1.4	8	0.963	*t* test	4.4 ± 0.8	6
Recording membrane potential (mV)	−59.8 ± 3.1	8	−61.2 ± 3.0	8	0.373	*t* test	−59.9 ± 1.9	6
2 s current step								
Persistent firing (neurons)	7 out of 7		9 out of 10				4 out of 4	
Initiation firing (Hz)	40.7 ± 5.1	7	32 (29; 34)	9	0.534	*U* test	33 (31; 35)	4
Persistent firing (Hz)	8.7 ± 2.3	7	7.4 ± 4.2	9	0.825	*U*	5.2 (4.6;	4

Note: Averaged data are given as mean ± *SD* or as median (P_{25}; P_{75}). *p* values for hepta-TRPC KO versus WT control (unpaired two-tailed *t* test or Mann–Whitney *U* test).
Abbreviations: LV, layer V; mEC, medial entorhinal cortex; TRPC, transient receptor potential canonical.

3.2 Persistent activity in TRPC hepta-KO mice

It cannot be excluded that the deleted channel subunits (TRPC1, TRPC4, and TRPC5) were functionally substituted by other members of the TRPC-family. Moreover, qPCR analysis using RNA isolated from the entorhinal, perirhinal, and postrhinal cortices indicates robust expression of other TRPC subtypes, particularly TRPC7, but also TRPC2, TRPC3, and TRPC6 (Figure 2a), that indeed might contribute to persistent firing of these neurons. We therefore repeated the experiments in cells from mice lacking expression of all seven Trpc genes (termed "hepta-TRPC KO," Figure S1 and Table S1, and Birnbaumer, 2015). qPCR analysis using RNA isolated from brain tissue showed that all TRPC subunits are absent in the hepta-TRPC KO mice (Figure 2b, Table 2). RMP of these neurons was −73.4 ± 5.4 mV (n = 11) and input resistance was 83 MΩ (median, P_{25} = 59 MΩ and P_{75} = 89 MΩ) (n = 11; recordings in the presence of CCh, CNQX, APV, and picrotoxin). Intrinsic properties of neurons are summarized in Table S2. We found that mEC LV neurons lacking all seven TRPC-channel subunits could indeed respond to a suprathreshold current step with persistent firing that is comparable to WT controls (Figure 3a, left; 11 out of 12 tested cells from 7 hepta-TRPC KO mice; see below for WT control values). The persistent activity relied on the activation of muscarinic receptors as its induction was completely blocked by atropine (n = 3; Figure 3a right). Similar to the above-described observations in TRPC1/4/5 KO mice, the plateau-potential that sustained persistent firing in hepta-TRPC KO mice displayed pronounced activity- and voltage-dependence (Figure 3b,c). Indeed, persistent firing could be elicited by a short stimulation from voltage levels less ~10 mV negative to spike threshold. At this potential, a 1 s spike train (32.9 ± 5.8 Hz) elicited sustained firing at a frequency of 6.7 ± 3.7 Hz (8 out of 11 cells). These values were not significantly different from similar experiments in WT control mice (stimulation-induced firing 37.4 ± 3.3 Hz, persistent firing 8.7 ± 2.3 Hz; n = 6; no difference between WT controls and hepta-TRPC KO, p = .113 for induced firing, p = .253 for persistent firing, t test; Figure 3d). RMP of neurons from WT control mice was more depolarized than RMP in hepta-TRPC KO mice (−64.9 ± 2.2 mV (n = 6) vs. −73.4 ± 5.4 mV (n = 11), p = .002, t test, measured in presence of CCh). In line with previous findings, frequency of persistent firing in hepta-TRPC KO mice correlated positively with frequency of spike trains during current-step injections (Figure 3e).

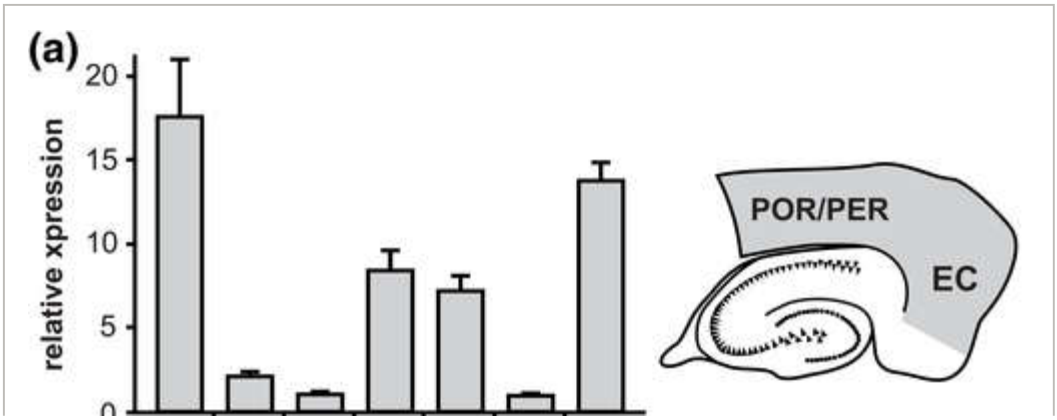

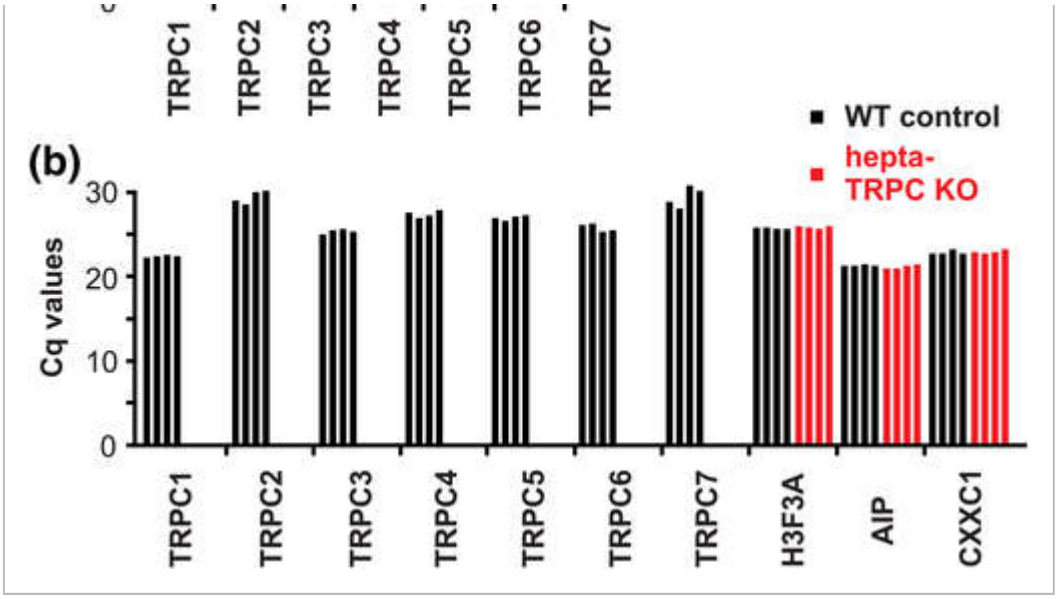

Figure 2

Open in figure viewer | PowerPoint

qPCR analysis of the Trpc subunits. (a) qPCR analysis of the Trpc subunits made by RNA isolated from the entorhinal cortex (EC) together with the perirhinal cortex (PER) and the postrhinal cortex (POR). Quantitative expression analysis was performed using high efficiency probe-based assays. Data are given as mean ± *SD* (four animals). (b) qPCR analysis using SYBR green I assays specifically designed to verify the respective Trpc deletion in brain tissue of hepta-TRPC KO mice. The primer efficiency varied between assays and accordingly the level of expression is displayed as Cq values. Each bar represents the value of one animal. qPCR, quantitative PCR; TRPC, transient receptor potential canonical [Color figure can be viewed at wileyonlinelibrary.com]

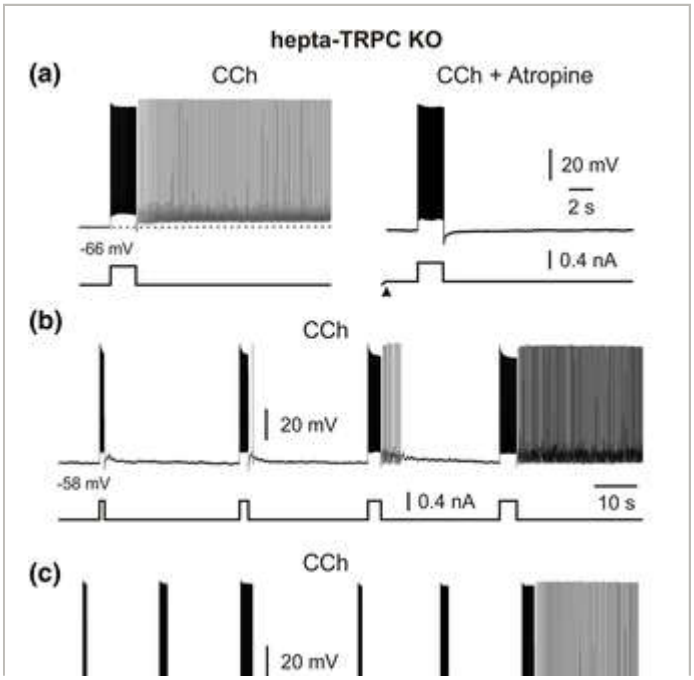

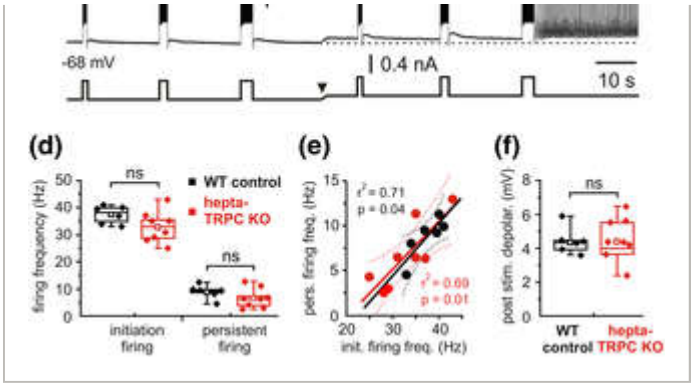

Figure 3

Open in figure viewer | PowerPoint

Muscarinic-dependent persistent activity in hepta-TRPC knockout mice. (a) CCh-induced persistent firing in mEC LV neuron in hepta-TRPC KO mice (left) and its complete block by the muscarinic antagonist atropine (1 μM; right). (b) Activity-dependence of persistent firing in hepta-TRPC KO mice. Responses of mEC LV neuron to depolarizing current steps of different duration. (c) Voltage-dependence of persistent firing in hepta-TRPC KO mice. Responses to depolarizing current steps at two different membrane potentials. The arrowhead indicates d.c. shift. (d) Box plots of firing frequency during 1 s current-step injection (initiation firing) and during persistent activity. No significant differences between WT control and hepta-TRPC KO mice were observed. (e) Frequency of persistent firing correlated positively with frequency of spike trains during current-step injections for WT control (black) and KO mice (red). Plotted data from (d). Dotted lines represent the 95% confidence intervals. (f) Box plots of membrane depolarization during persistent firing for WT control and KO mice. Box plots indicating median, 25th and 75th percentiles and individual values. Whiskers show 5th and 95th percentiles, squares indicate mean. ns, not significant, *t* test. All recordings were obtained during blockade of neurotransmission with CNQX, APV, and picrotoxin. APV, DL-2-amino-5-phosphonovaleric acid; CCh, carbachol; CNQX, 6-cyano-7-nitroquinoxaline-2,3-dione; LV, layer V; mEC, medial entorhinal cortex; TRPC, transient receptor potential canonical [Color figure can be viewed at wileyonlinelibrary.com]

The marked poststimulus membrane depolarization underlying the persistent firing was also not significantly different between WT control and hepta-TRPC KO mice (4.4 ± 0.8 mV (n = 6) vs. 4.4 ± 1.4 mV (n = 8), p = .963, t test; Figure 3f). A 2-s spike train at 32 Hz (median) elicited a post stimulus membrane depolarization of 5.0 ± 2.2 mV and sustained firing at a frequency of 7.4 ± 4.2 Hz (n = 9 for all values, 9/10 tested neurons). Quantitative parameters of persistent activity were not statistically different between hepta-TRPC KO and WT control mice (Table 3). Similar to TRPC1/4/5 KO mice, persistent firing in hepta-TRPC KO mice could be elicited by a 0.2 s current step (1/3 tested neurons; Figure 4a). Analogues to our previous observations (Egorov,

Hamam, et al., 2002), persistent firing could be reversibly turned off by prolonged membrane hyperpolarization for 6–12 s to below ~ −80 mV (Figure 4b).

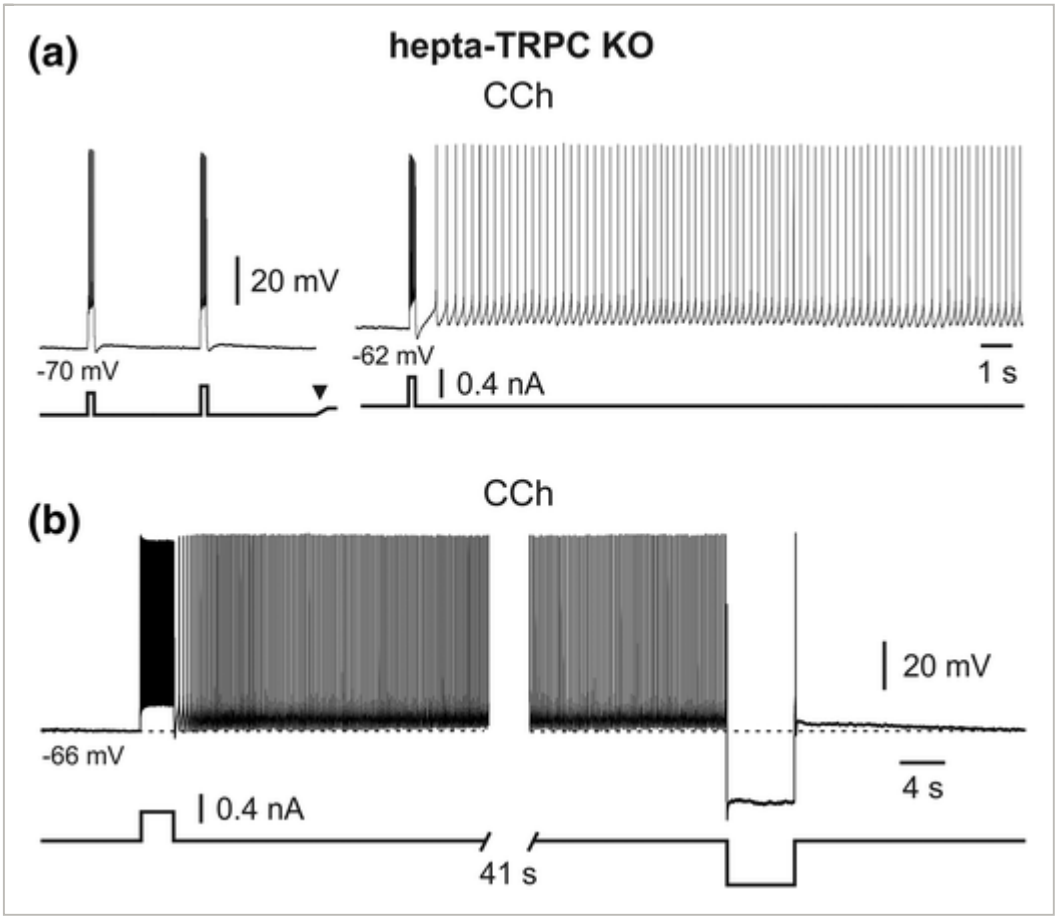

Figure 4

Open in figure viewer | PowerPoint

Induction and termination of persistent firing in hepta-TRPC knockout mice. (a) An example of a neurons that showed voltage-dependent persistent firing in response a brief stimulus (0.2 s, +0.4 nA). The arrowhead indicates d.c. shift. (b) Persistent firing termination by prolonged hyperpolarizing current pulse (6 s, −0.6 nA). All recordings were performed in the presence of CCh, CNQX, APV, and picrotoxin. APV, DL-2-amino-5-phosphonovaleric acid; CCh, carbachol; CNQX, 6-cyano-7-nitroquinoxaline-2,3-dione; TRPC, transient receptor potential canonical

3.3 Graded persistent activity in TRPC hepta-KO mice

Medial EC LV neurons generate graded persistent activity upon repetitive stimulation (Egorov, Hamam, et al., 2002; Fransén et al., 2006; Reboreda et al., 2007). We tested this behavior in cells from hepta-TRPC KO mice. As illustrated in Figure 5a, repetitive application of an activating current step gave rise to graded increases of sustained discharge rates (eight neurons from six mice; three to seven levels following repetitive stimulation with a 1–4 s depolarizing step). The

maximum persistent firing frequency induced in this manner in hepta-TRPC KO mice was 9 Hz (median, $n = 18$, minimal value: 6.3 Hz, maximal value: 19 Hz). In addition, repetitive application of hyperpolarizing current pulse steps led to graded decreases in firing rate ($n = 3$, Figure 5b). Stimulus durations of at least 6–8 s were required for this graded decrease in persistent firing rate.

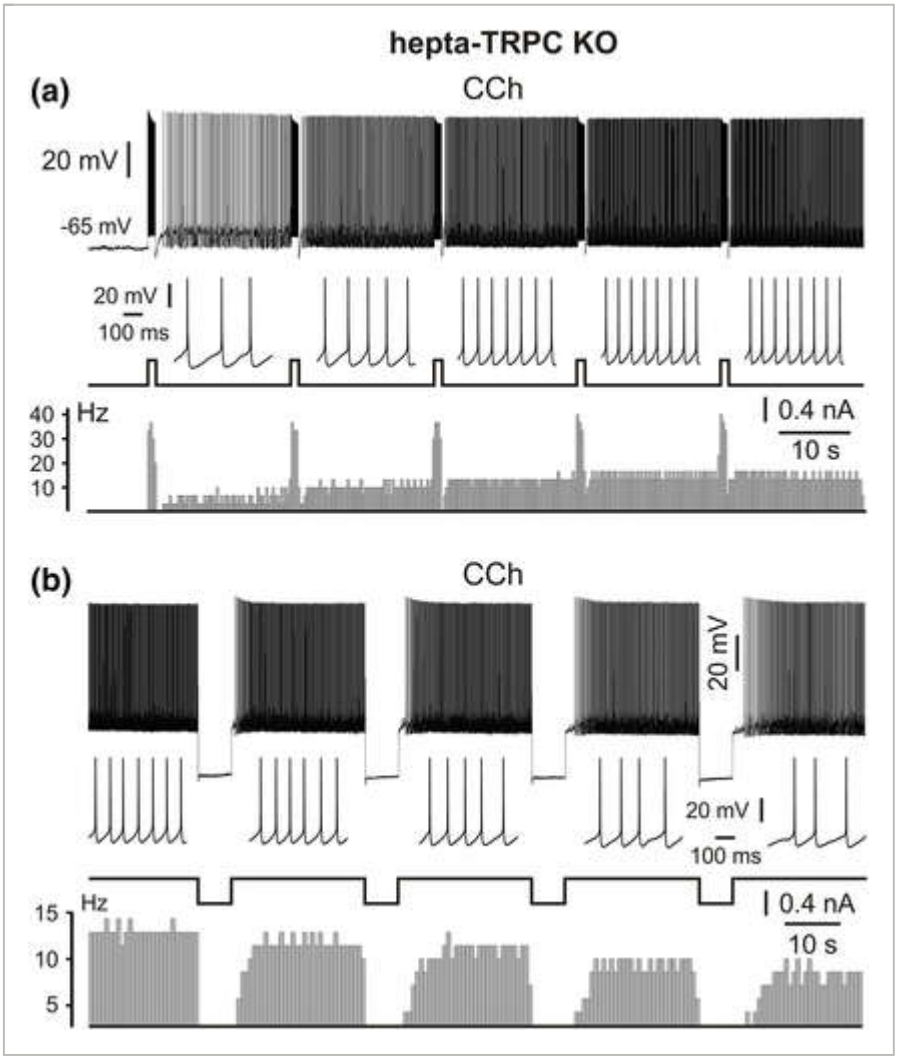

Figure 5

Open in figure viewer | PowerPoint

Graded persistent activity in hepta-TRPC knockout mice. (a) Repetitive stimulation with a 1 s depolarizing current step gives rise to four distinct increases of stable discharge rate in mEC LV neuron in hepta-TRPC KO mice. (b) Repetitive application of 6 s hyperpolarizing steps gives rise to discrete decreases of firing rate. Short intervals of firing are shown at an expanded time scale for each level below voltage traces. The lower diagrams correspond to the peristimulus histograms (bin width in (a) and (b): 300 ms and 700 ms, respectively). All recordings were performed in the presence of CCh, CNQX, APV, and picrotoxin. APV, DL-2-amino-5-phosphonovaleric acid; CCh,

carbachol; CNQX, 6-cyano-7-nitroquinoxaline-2,3-dione; LV, layer V; mEC, medial entorhinal cortex; TRPC, transient receptor potential canonical

In three out of eight neurons in hepta-TRPC KO mice repetitive depolarizing current steps initially gave rise to graded increases of firing rate followed by a decrease in firing frequency and, finally, termination (Figure 6a). This sequence could be repeated after ~100 s of silence, suggesting an activity- (e.g., calcium-) dependent mechanism of inactivation. This behavior is well compatible with the inverted U-shape of the Ca^{2+} dependence of persistent firing in mEC cells from WT rats (Zhang et al., 2011). In these experiments, Zhang and colleagues tested effects of intracellular Ca^{2+} concentration ($[Ca^{2+}]_i$) on the persistent spiking activity in mEC LV neurons by clamping $[Ca^{2+}]_i$ with BAPTA in the patch pipette. The authors found that Ca^{2+} influx from the extracellular space is required to establish an optimal window of $[Ca^{2+}]_i$ (70–500 nM) for CCh-evoked persistent activity. When $[Ca^{2+}]_i$ was maintained at a low (20 nM) or high (1 mM) levels, CCh-evoked persistent firing in response to depolarizing current pulses was absent. Persistent firing relied on the activation of muscarinic receptors, as its induction was completely blocked after adding atropine (Figure 6b).

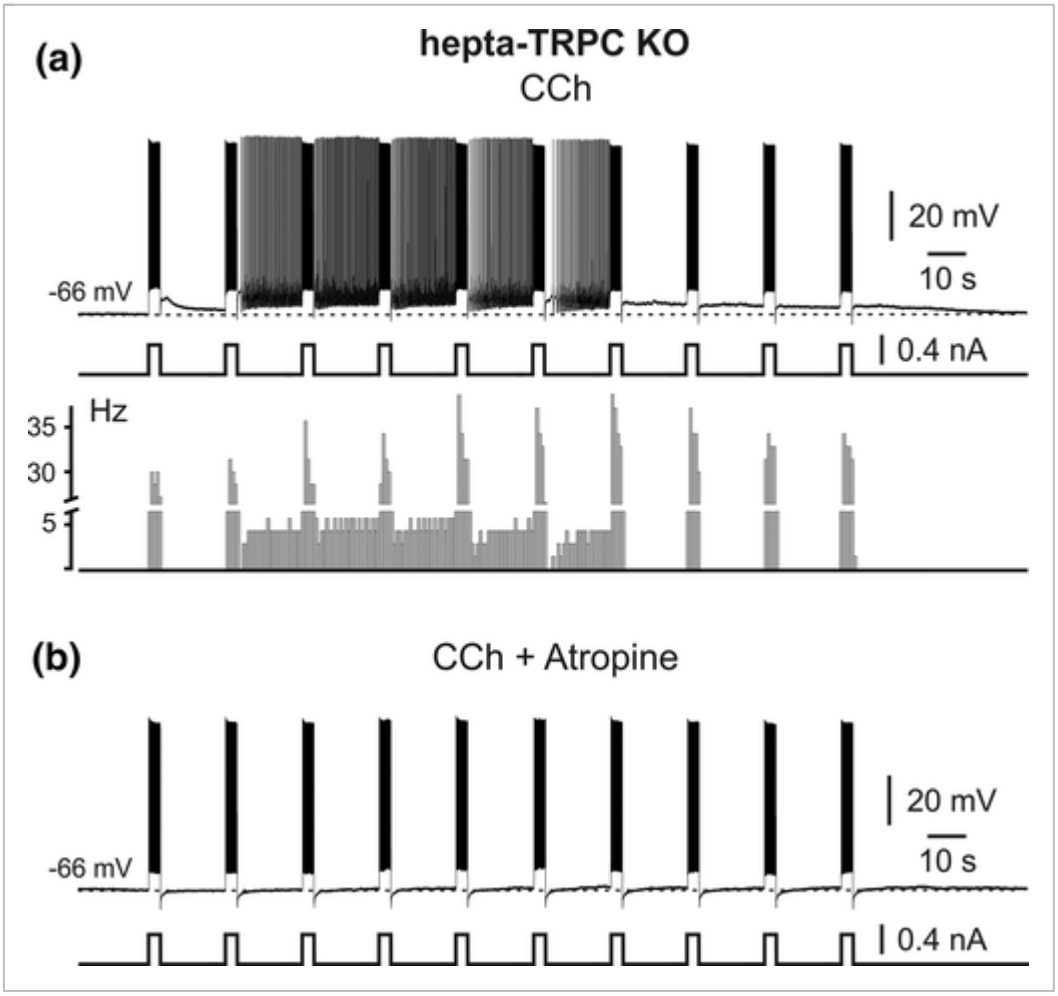

Figure 6

Open in figure viewer | PowerPoint

Activity dependent modulation of graded persistent firing in hepta-TRPC knockout mice. (a) Specimen trace showing that repetitive depolarizing current step gives initially increases of stable discharge rate followed, however, by its discrete decreases and full termination. The lower diagram correspond to the peristimulus histograms (bin width 700 ms). (b) Repetitive stimulation in same neuron after adding atropine. Recording was performed in the presence of CCh, CNQX, APV, and picrotoxin. APV, DL-2-amino-5-phosphonovaleric acid; CCh, carbachol; CNQX, 6-cyano-7-nitroquinoxaline-2,3-dione; TRPC, transient receptor potential canonical

4 DISCUSSION

Persistent and graded persistent firing during a delayed response task, in which the animal is required to keep information about a sensory signal across a delay period between the stimulus and the behavioral response, may represent a cellular analog of working memory (Zylberberg & Strowbridge, 2017). In brain slices, persistent activity or slow afterdepolarization (sADP), following spike firing during activation of muscarinic acetylcholine receptors have been reported in many types of cortical neurons, including pyramidal cells of the EC, hippocampus, and neocortex (Egorov, Hamam, et al., 2002; Knauer et al., 2013; Lei et al., 2014).

In this study, we investigated the potential contribution of TRPC channels to generation of persistent activity in mEC LV neurons. Involvement of TRPC channels in cholinergic persistent activity has been suggested by various observations (including our own). This was assumed, however, based on nonspecific pharmacological experiments as well as peptides that interfere with TRP channel functions (Al-Yahya et al., 2003; Reboreda et al., 2011; Tai, Hines, Choi, & MacVicar, 2011; Zhang et al., 2011). Previous studies have proposed that the nonselective cation current underlying sustained firing in the mEC is mediated by heteromultimeric TRPC channels containing TRPC1, TRPC4, or/and TRPC5 subunits (Zhang et al., 2011). Indeed, these subunits are expressed in the EC (von Bohlen und Halbach, Hinz, Unsicker, & Egorov, 2005). We here report recordings from individual mEC LV neurons obtained from mice lacking any TRPC1-, TRPC4-, and TRPC5-containing channels (Bröker-Lai et al., 2017) or a mouse line lacking all seven TRPC subtypes (Birnbaumer, 2015) that might contribute to formation of alternative TRPC heteromers. Our results lead, however, to the conclusion that TRPC channels are not necessary for persistent firing in the EC. We note that some hepta-TRPC KO neurons showed only transient plateau potentials but no persistent firing (see Table 3). This is, however, possibly due to inter-cell variance or to small differences in intrinsic neuronal properties which impair induction of persistent activity. In any case, hepta-TRPC KO neurons are clearly able to express persistent activity.

The potential involvement of TRPC channels to persistent firing or sADP in neocortical neurons has remained a controversial issue, and the ability of TRP proteins to form multimers complicates testing this hypothesis. It has been reported that expression of dominant negative TRPC subunits can attenuate sADP responses in prefrontal cortex neurons (Yan, Villalobos, & Andrade, 2009). However, genetic deletion of several TRPC subunits, including TRPC1, TRPC5, and TRPC6 (single KOs), or both TRPC5 and TRPC6 together (double KO), failed to reduce the amplitude of cholinergic sADPs in LV pyramidal neurons of the mouse medial prefrontal cortex (Dasari, Abramowitz, Birnbaumer, & Gulledge, 2013). Indeed, besides TRPC, other subfamily member of TRP channels, that are expressed in the brain (Sawamura, Shirakawa, Nakagawa, Mori, & Kaneko, 2017), could underlie persistent activity in cortical neurons. For instance, the TRP melastatin 5 channel (TRPM5) contributes importantly to the sADP in the mouse prefrontal cortex (Lei et al., 2014). By examining animals in which TRPM4 and TRPM5 channels were genetically deleted either alone or in combination this study further showed that TRPM5 but not TRPM4 channels are involved in the generation of the sADP in LV neurons. Nevertheless, as a significant sADP was still observed in TRPM4/5 double KO mice, the sADP must mediated by more than one type of ion channel (Lei et al., 2014). Pharmacology-based approaches suggest involvement of TRPM channels (particularly Ca^{2+} activated cation channel TRPM4) (Nilius et al., 2003) in the regulation of neuronal excitability in diverse cell types. Thus, TRPM4 and TRPM5 are the ion channels underlying I_{CAN} in preBötzinger complex neurons during inspiratory burst activity (Crowder et al., 2007). TRPM2/TRPM4 channels are involved in generation of bursting activity in dopamine neurons of the substantia nigra (Mrejeru, Wei, & Ramirez, 2011). In the mEC TRPM (probably TRPM4) mediates I_{CAN} which is responsible for the generation of hyperexcitable bursts at proximal dendrites of LV neurons. In the same preparation, antagonists of TRPC did not affect bursting behavior (Lin, Combe, & Gasparini, 2017). These data show a limited contribution of TRPC channels to the regulation of neuronal excitability in mEC LV neurons, in line with our current results. In contrast, TRPM channels may be involved in generation of graded persistent firing in the mEC.

In addition to I_{CAN}, different inward or outward currents which are active near the resting potential could support intrinsic persistent activity (Debanne, Inglebert, & Russier, 2018; Zylberberg & Strowbridge, 2017). Thus, using both biophysical and pharmacological assays, Cui and Strowbridge nicely demonstrated that in neocortical neurons charbachol mediated persistent firing may result from the modulation of ether-á-Go-Go related gene (ERG) K^+ channels (Cui & Strowbridge, 2018). Accordingly, ERG channels mediate a leak potassium current which is downregulated by calcium entry induced by repetitive spiking.

There is convergent evidence showing involvement of TRPC channels in cognitive functions. Therefore, TRPC1/4/5 KO mice (i.e., animals that we used in our current study) display deficits in spatial working memory and flexible spatial relearning as demonstrated in hippocampus-

specific tasks, while spatial reference memory assessed using the Morris water maze is unaltered (Bröker-Lai et al., 2017). Deletion of the TRPC1 gene alone impairs spatial working memory and fear memory (Lepannetier et al., 2018). Mice lacking TRPC4 or TRPC5 channels have been shown to exhibit less anxious behaviors (decreased innate fear) than their WT counterparts (Riccio et al., 2009, 2014). In contrast, targeted knockdown of TRPC3 channel in the hippocampus enhanced contextual fear conditioning (Neuner et al., 2015). Nevertheless, the role of TRPC channels in memory-related functions and particularly the link between sustained firing activity and working memory are still not completely understood. Our present findings show that one potential mechanisms of working memory, persistent neuronal firing, is not related to the presence of any of the TRPC proteins, at least in mEC neurons. Further studies will need to define the molecular identity of the calcium-activated nonselective cation channels underlying persistent firing in the EC.

ACKNOWLEDGMENTS

This work was supported by the Deutsche Forschungsgemeinschaft (SFB 1134, A01 to A.V.E. and A.D. and SFB-TRR 152, P07, P21, SFB 1118, B02, FOR 2289, P02 to M.F.) and by the Intramural Research Program of the NIH (project Z01-ES-101684 to L.B.). We thank Prof. Klaus Groschner and Patrick Wiedner (University of Graz) for great help with transgenic animals. We also thank Yoko Oguchi and Christin Matka for the expert assistance in the qPCR analysis and Dr. Angela Wirth for her help during preparation of this manuscript.

CONFLICT OF INTEREST

The authors declare that they have no conflict of interest.

Supporting Information

Filename	Description
hipo23094-sup-0001-AppendixS1.pdf PDF document, 1.5 MB	**Appendix S1**: Supporting Information

Please note: The publisher is not responsible for the content or functionality of any supporting information supplied by the authors. Any queries (other than missing content) should be directed to the corresponding author for the article.

REFERENCES

Al-Yahya, E., Hamel, E., Kennedy, T. E., Alonso, A. A., & Egorov, A. V. (2003). Persistent activity in entorhinal cortex neurons induced by muscarinic and metabotropic glutamate receptor activation and its dependence on TRP channels. Society for Neuroscience Abstract, 377.5.
Google Scholar

Birnbaumer, L. (2015). From GTP and G proteins to TRPC channels: A personal account. *Journal of Molecular Medicine (Berlin)*, **93**(9), 941– 553.
Crossref | CAS | PubMed | Web of Science® | Google Scholar

Bröker-Lai, J., Kollewe, A., Schindeldecker, B., Pohle, J., Nguyen Chi, V., Mathar, I., … Freichel, M. (2017). Heteromeric channels formed by TRPC1, TRPC4 and TRPC5 define hippocampal synaptic transmission and working memory. *EMBO Journal*, **36**(18), 2770– 2789.
Wiley Online Library | CAS | PubMed | Web of Science® | Google Scholar

Crowder, E. A., Saha, M. S., Pace, R. W., Zhang, H., Prestwich, G. D., & Del Negro, C. A. (2007). Phosphatidylinositol 4,5-bisphosphate regulates inspiratory burst activity in the neonatal mouse preBötzinger complex. *Journal of Physiology*, **582**, 1047– 1058.
Wiley Online Library | CAS | PubMed | Web of Science® | Google Scholar

Cui, E. D., & Strowbridge, B. W. (2018). Modulation of ether-à-go-go related gene (ERG) current governs intrinsic persistent activity in rodent neocortical pyramidal cells. *The Journal of Neuroscience*, **38**(2), 423– 440.
Crossref | CAS | PubMed | Web of Science® | Google Scholar

Dasari, S., Abramowitz, J., Birnbaumer, L., & Gulledge, A. T. (2013). Do canonical transient receptor potential channels mediate cholinergic excitation of cortical pyramidal neurons? *Neuroreport*, **24**(10), 550– 554.
Crossref | PubMed | Web of Science® | Google Scholar

Debanne, D., Inglebert, Y., & Russier, M. (2018). Plasticity of intrinsic neuronal excitability. *Current Opinion in Neurobiology*, **54**, 73– 82.
Crossref | PubMed | Web of Science® | Google Scholar

Dietrich, A., Kalwa, H., Storch, U., Mederos y Schnitzler, M., Salanova, B., Pinkenburg, O., … Gudermann, T. (2007). Pressureinduced and store-operated cation influx in vascular smooth muscle cells is independent of TRPC1. *Pflügers Archiv*, **455**(3), 465– 477.
Crossref | CAS | PubMed | Web of Science® | Google Scholar

Dietrich, A., Mederos Y Schnitzler, M., Gollasch, M., Gross, V., Storch, U., Dubrovska, G., … Birnbaumer, L. (2005). Increased vascular smooth muscle contractility in TRPC6−/− mice. *Molecular and Cellular Biology*, **25**(16), 6980– 6989.
Crossref | CAS | PubMed | Web of Science® | Google Scholar

Egorov, A. V., Hamam, B. N., Fransén, E., Hasselmo, M. E., & Alonso, A. A. (2002). Graded persistent activity in entorhinal cortex neurons. *Nature*, **420**(6912), 173– 178.
Crossref | CAS | PubMed | Web of Science® | Google Scholar

Egorov, A. V., Heinemann, U., & Müller, W. (2002). Differential excitability and voltage-dependent Ca2+ signalling in two types of medial entorhinal cortex layer V neurons. *European Journal of Neuroscience*, **16**(7), 1305– 1312.
Wiley Online Library | PubMed | Web of Science® | Google Scholar

Egorov, A. V., Unsicker, K., & von Bohlen und Halbach, O. (2006). Muscarinic control of graded persistent activity in lateral amygdala neurons. *European Journal of Neuroscience*, **24**(11), 3183– 3194.
Wiley Online Library | PubMed | Web of Science® | Google Scholar

Fransén, E., Tahvildari, B., Egorov, A. V., Hasselmo, M. E., & Alonso, A. A. (2006). Mechanism of graded persistent cellular activity in entorhinal cortex layer V neurons. *Neuron*, **49**(5), 735– 746.
Crossref | CAS | PubMed | Web of Science® | Google Scholar

Freichel, M., Suh, S. H., Pfeifer, A., Schweig, U., Trost, C., Weissgerber, P., … Nilius, B. (2001). Lack of an endothelial store-operated Ca2+ current impairs agonist-dependent vasorelaxation in TRP4−/− mice. *Nature Cell Biology*, **3**(2), 121– 127.
Crossref | CAS | PubMed | Web of Science® | Google Scholar

Funahashi, S., Bruce, C. J., & Goldman-Rakic, P. S. (1989). Mnemonic coding of visual space in the monkey's dorsolateral prefrontal cortex. *Journal of Neurophysiology*, **61**(2), 331– 349.
Crossref | CAS | PubMed | Web of Science® | Google Scholar

Haas, H. L., Schaerer, B., & Vosmansky, M. (1979). A simple perfusion chamber for the study of nervous tissue slices in vitro. *Journal of Neuroscience Methods*, **1**(4), 323– 325.
Crossref | CAS | PubMed | Web of Science® | Google Scholar

Hamam, B. N., Kennedy, T. E., Alonso, A., & Amaral, D. G. (2000). Morphological and electrophysiological characteristics of layer V neurons of the rat medial entorhinal cortex. *The Journal of Comparative Neurology*, **418**(4), 457– 472.
Wiley Online Library | CAS | PubMed | Web of Science® | Google Scholar

Hartmann, J., Dragicevic, E., Adelsberger, H., Henning, H. A., Sumser, M., Abramowitz, J., … Konnerth, A. (2008). TRPC3 channels are required for synaptic transmission and motor coordination. *Neuron*, **59**(3), 392– 398.
Crossref | CAS | PubMed | Web of Science® | Google Scholar

Harvey, C. D., Coen, P., & Tank, D. W. (2012). Choice-specific sequences in parietal cortex during a virtual-navigation decision task. *Nature*, **484**(7392), 62– 68.

Crossref | CAS | PubMed | Web of Science® | Google Scholar

Jochems, A., & Yoshida, M. (2013). Persistent firing supported by an intrinsic cellular mechanism in hippocampal CA3 pyramidal cells. *European Journal of Neuroscience*, **38**(2), 2250– 2259.
Wiley Online Library | CAS | PubMed | Web of Science® | Google Scholar

Kamiński, J., Sullivan, S., Chung, J. M., Ross, I. B., Mamelak, A. N., & Rutishauser, U. (2017). Persistently active neurons in human medial frontal and medial temporal lobe support working memory. *Nature Neuroscience*, **20**(4), 590– 601.
Crossref | CAS | PubMed | Web of Science® | Google Scholar

Knauer, B., Jochems, A., Valero-Aracama, M. J., & Yoshida, M. (2013). Long-lasting intrinsic persistent firing in rat CA1 pyramidal cells: A possible mechanism for active maintenance of memory. *Hippocampus*, **23**(9), 820– 831.
Wiley Online Library | CAS | PubMed | Web of Science® | Google Scholar

Larimer, P., & Strowbridge, B. W. (2010). Representing information in cell assemblies: Persistent activity mediated by semilunar granule cells. *Nature Neuroscience*, **13**(2), 213– 222.
Crossref | CAS | PubMed | Web of Science® | Google Scholar

Lei, Y. T., Thuault, S. J., Launay, P., Margolskee, R. F., Kandel, E. R., & Siegelbaum, S. A. (2014). Differential contribution of TRPM4 and TRPM5 nonselective cation channels to the slow afterdepolarization in mouse prefrontal cortex neurons. *Frontiers in Cellular Neuroscience*, **8**, 267.
Crossref | PubMed | Web of Science® | Google Scholar

Lepannetier, S., Gualdani, R., Tempesta, S., Schakman, O., Seghers, F., Kreis, A., … Gailly, P. (2018). Activation of TRPC1 channel by metabotropic glutamate receptor mGluR5 modulates synaptic plasticity and spatial working memory. *Frontiers in Cellular Neuroscience*, **12**, 318.
Crossref | PubMed | Web of Science® | Google Scholar

Lin, E. C., Combe, C. L., & Gasparini, S. (2017). Differential contribution of Ca2+−dependent mechanisms to hyperexcitability in layer V neurons of the medial entorhinal cortex. *Frontiers in Cellular Neuroscience*, **11**, 182.
Crossref | Web of Science® | Google Scholar

MacDonald, C. J., Lepage, K. Q., Eden, U. T., & Eichenbaum, H. (2011). Hippocampal “time cells” bridge the gap in memory for discontiguous events. *Neuron*, **71**(4), 737– 749.
Crossref | CAS | PubMed | Web of Science® | Google Scholar

Major, G., & Tank, D. (2004). Persistent neural activity: Prevalence and mechanisms. *Current Opinion in Neurobiology*, **14**(6), 675– 684.
Crossref | CAS | PubMed | Web of Science® | Google Scholar

Miller, E. K., Erickson, C. A., & Desimone, R. (1996). Neural mechanisms of visual working memory in prefrontal cortex of the macaque. *Journal of Neuroscience*, **16**(16), 5154– 5167.
Crossref | CAS | PubMed | Web of Science® | Google Scholar

Montell, C., Birnbaumer, L., & Flockerzi, V. (2002). The TRP channels, a remarkably functional family. *Cell*, **108**(5), 595– 598.
Crossref | CAS | PubMed | Web of Science® | Google Scholar

Mrejeru, A., Wei, A., & Ramirez, J. M. (2011). Calcium-activated non-selective cation currents are involved in generation of tonic and bursting activity in dopamine neurons of the substantia nigra pars compacta. *Journal of Physiology*, **589**, 2497– 2514.
Wiley Online Library | CAS | PubMed | Web of Science® | Google Scholar

Navaroli, V. L., Zhao, Y., Boguszewski, P., & Brown, T. H. (2012). Muscarinic receptor activation enables persistent firing in pyramidal neurons from superficial layers of dorsal perirhinal cortex. *Hippocampus*, **22**(6), 1392– 1404.
Wiley Online Library | CAS | PubMed | Web of Science® | Google Scholar

Neuner, S. M., Wilmott, L. A., Hope, K. A., Hoffmann, B., Chong, J. A., Abramowitz, J., … Kaczorowski, C. C. (2015). TRPC3 channels critically regulate hippocampal excitability and contextual fear memory. *Behavioural Brain Research*, **281**, 69– 77.
Crossref | CAS | PubMed | Web of Science® | Google Scholar

Nilius, B., Prenen, J., Droogmans, G., Voets, T., Vennekens, R., Freichel, M., … Flockerzi, V. (2003). Voltage dependence of the Ca^{2+}-activated cation channel TRPM4. *Journal of Biological Chemistry*, **278**(33), 30813– 30820.
Crossref | CAS | PubMed | Web of Science® | Google Scholar

Pastalkova, E., Itskov, V., Amarasingham, A., & Buzsaki, G. (2008). Internally generated cell assembly sequences in the rat hippocampus. *Science*, **321**(5894), 1322– 1327.
Crossref | CAS | PubMed | Web of Science® | Google Scholar

Perez-Leighton, C. E., Schmidt, T. M., Abramowitz, J., Birnbaumer, L., & Kofuji, P. (2011). Intrinsic phototransduction persists in melanopsin-expressing ganglion cells lacking diacylglycerol-sensitive TRPC subunits. *European Journal of Neuroscience*, **33**(5), 856– 867.
Wiley Online Library | PubMed | Web of Science® | Google Scholar

Phelan, K. D., Shwe, U. T., Abramowitz, J., Wu, H., Rhee, S. W., Howell, M. D., … Zheng, F. (2013). Canonical transient receptor channel 5 (TRPC5) and TRPC1/4 contribute to seizure and excitotoxicity by distinct cellular mechanisms. *Molecular Pharmacology*, **83**(2), 429– 438.
Crossref | CAS | PubMed | Web of Science® | Google Scholar

Ramsey, I. S., Delling, M., & Clapham, D. E. (2006). An introduction to TRP channels. *Annual Review of Physiology*, **68**, 619– 647.
Crossref | CAS | PubMed | Web of Science® | Google Scholar

Reboreda, A., Jiménez-Díaz, L., & Navarro-López, J. D. (2011). TRP channels and neural persistent activity. *Advances in Experimental Medicine and Biology*, **704**, 595– 613.
Crossref | CAS | PubMed | Web of Science® | Google Scholar

Reboreda, A., Raouf, R., Alonso, A., & Séguéla, P. (2007). Development of cholinergic modulation and graded persistent activity in layer v of medial entorhinal cortex. *Journal of Neurophysiology*, **97**(6), 3937– 3947.
Crossref | CAS | PubMed | Web of Science® | Google Scholar

Riccio, A., Li, Y., Moon, J., Kim, K. S., Smith, K. S., Rudolph, U., … Clapham, D. E. (2009). Essential role for TRPC5 in amygdala function and fear-related behavior. *Cell*, **137**(4), 761– 772.
Crossref | CAS | PubMed | Web of Science® | Google Scholar

Riccio, A., Li, Y., Tsvetkov, E., Gapon, S., Yao, G. L., Smith, K. S., … Clapham, D. E. (2014). Decreased anxiety-like behavior and G q/11-dependent responses in the amygdala of mice lacking TRPC4 channels. *The Journal of Neuroscience*, **34**(10), 3653– 3667.
Crossref | CAS | PubMed | Web of Science® | Google Scholar

Romo, R., Brody, C. D., Hernández, A., & Lemus, L. (1999). Neuronal correlates of parametric working memory in the prefrontal cortex. *Nature*, **399**(6735), 470– 473.
Crossref | CAS | PubMed | Web of Science® | Google Scholar

Roth, F. C., Beyer, K. M., Both, M., Draguhn, A., & Egorov, A. V. (2016). Downstream effects of hippocampal sharp wave ripple oscillations on medial entorhinal cortex layer V neurons in vitro. *Hippocampus*, **26**(12), 1493– 1508.
Wiley Online Library | PubMed | Web of Science® | Google Scholar

Sawamura, S., Shirakawa, H., Nakagawa, T., Mori, Y., & Kaneko, S. (2017). Chapter 16. TRP channels in the brain: What are they there for? In T. L. R. Emir (Ed.), *Neurobiology of TRP channels* (2nd ed.). Boca Raton, FL: CRC Press.
Google Scholar

Stowers, L., Holy, T. E., Meister, M., Dulac, C., & Koentges, G. (2002). Loss of sex discrimination and male-male aggression in mice deficient for TRP2. *Science*, **295**(5559), 1493– 1500.
Crossref | CAS | PubMed | Web of Science® | Google Scholar

Tahvildari, B., Alonso, A. A., & Bourque, C. W. (2008). Ionic basis of ON and OFF per-sistent activity in layer III lateral entorhinal cortical principal neurons. *Journal of Neurophysiology*, **99**(4), 2006– 2011.
Crossref | PubMed | Web of Science® | Google Scholar

Tahvildari, B., Fransén, E., Alonso, A. A., & Hasselmo, M. E. (2007). Switching between "On" and "Off" states of persistent activity in lateral entorhinal layer III neurons. *Hippocampus*, **17**(4), 257– 263.
Wiley Online Library | CAS | PubMed | Web of Science® | Google Scholar

Tai, C., Hines, D. J., Choi, H. B., & MacVicar, B. A. (2011). Plasma membrane insertion of TRPC5 channels contributes to the cholinergic plateau potential in hippocampal CA1 pyramidal neurons. *Hippocampus*, **21**(9), 958– 967.
Wiley Online Library | CAS | PubMed | Web of Science® | Google Scholar

von Bohlen und Halbach, O., Hinz, U., Unsicker, K., & Egorov, A. V. (2005). Distribution of TRPC1 and TRPC5 in medial temporal lobe structures of mice. *Cell and Tissue Research*, **322**(2), 201– 206.
Crossref | PubMed | Web of Science® | Google Scholar

Wu, L. J., Sweet, T. B., & Clapham, D. E. (2010). International Union of Basic and Clinical Pharmacology. LXXVI. Current progress in the mammalian TRP ion channel family. *Pharmacological Reviews*, **62**(3), 381– 404.
Crossref | CAS | PubMed | Web of Science® | Google Scholar

Xue, T., Do, M. T., Riccio, A., Jiang, Z., Hsieh, J., Wang, H. C., … Yau, K. W. (2011). Melanopsin signalling in mammalian iris and retina. *Nature*, **479**(7371), 67– 73.
Crossref | CAS | PubMed | Web of Science® | Google Scholar

Yan, H. D., Villalobos, C., & Andrade, R. (2009). TRPC channels mediate a muscarinic receptor-induced afterdepolarization in cerebral cortex. *The Journal of Neuroscience*, **29**(32), 10038– 10046.
Crossref | CAS | PubMed | Web of Science® | Google Scholar

Yoshida, M., & Hasselmo, M. E. (2009). Persistent firing supported by an intrinsic cellular mechanism in a component of the head direction system. *Journal of Neuroscience*, **29**(15), 4945– 4952.
Crossref | CAS | PubMed | Web of Science® | Google Scholar

Zhang, Z., Reboreda, A., Alonso, A., Barker, P. A., & Séguéla, P. (2011). TRPC channels underlie cholinergic plateau potentials and persistent activity in entorhinal cortex. *Hippocampus*, **21**(4), 386– 397.
Wiley Online Library | CAS | PubMed | Web of Science® | Google Scholar

Zylberberg, J., & Strowbridge, B. W. (2017). Mechanisms of persistent activity in cortical circuits: Possible neural substrates for working memory. *Annual Review of Neuroscience*, **40**, 603– 627.
Crossref | CAS | PubMed | Web of Science® | Google Scholar